Available online at www.sciencedirect.com

ScienceDirect

Procedia CIRP 58 (2017) 239 – 244

www.elsevier.com/locate/procedia

16th CIRP Conference on Modelling of Machining Operations

Modelling of pocket milling operation considering cutting forces and CNC control inputs

Abdullah Ozcan[a]*, Edouard Rivière-Lorphèvre[a], Hoai Nam Huynh[b], François Ducobu[a], Olivier Verlinden[b], Enrico Filippi[a]

[a]*University of Mons, Machine Design and Production Engineering, Place du parc 20, 7000 Mons, Belgium*
[b]*University of Mons, Theoretical Mechanics, Dynamics and Vibrations, Place du parc 20, 7000 Mons, Belgium*

* Abdullah Ozcan. Tel.: +32-65-374552; fax: +32-65-374545. *E-mail address:* abdullah.ozcan@umons.ac.be

Abstract

Machining of large pocket is a key issue for the production of aerospace parts. The optimization of this phase may lead to interesting cost reduction.
This paper will study the prediction of the cutting forces acting on a milling tool while machining the corner of a pocket and the impact of the general behavior of the machine tool on the process time.
These aspects are combined in a simulation framework at a macroscopic level. Some simulation results are presented and commented. This work can be used to optimize the cutting condition and tested on various toolpath strategies.

Peer-review under responsibility of the scientific committee of The 16th CIRP Conference on Modelling of Machining Operations

Keywords: CNC, machine-tool, force

1. Introduction

In part manufacturing, reducing the production costs and optimizing the manufacturing time is an important issue. However, the produced part quality should not be neglected. Thus, the cost quality ratio should always be as low as possible [1].

In order to achieve that, simulation of manufacturing techniques has an increasing role for industrial applications. These techniques allow realization of virtual prototyping stage which gives access to a large flexibility in optimization of manufacturing parameters. Thus, the manufacturing process can be freed, partially or completely, from an expensive physical prototyping stage.

There are many works which focus on the simulation of the machining process. These works can be classified as follows:

- Toolpath generation by taking into account kinematic constraints [2, 3, 4];
- Modelling of different entities of a CNC (motor, amplifiers, guideways, …) [5, 6];
- Controller stage [7, 8];
- Machining process (prediction of cutting forces) [5, 9].

The simulation of the actual behavior of the machine tool plays a key role in order to predict an optimal toolpath for a given operation. Indeed, the shortest toolpath is not necessarily the fastest one. The physical limits of the machine in terms of maximum acceleration or jerk for example reduce the feedrate that can be reached along the toolpath [10, 11, 12].

In this context, this work presents a simulation framework developed for the simulation of CNC machining at a macroscopic level. The developed framework combines [13]:

- A multibody simulation library which takes into account the behavior of the machine tool and its control [14, 15], presented in section 2;
- A mechanistic model used to predict the cutting forces, detailed in section 3.

Peer-review under responsibility of the scientific committee of The 16th CIRP Conference on Modelling of Machining Operations
doi:10.1016/j.procir.2017.03.187

In section 4, the results of 90° corner milling simulation, with cutting forces considered, are presented and commented.

2. CNC axes dynamic model

2.1. Multibody simulation library

The multibody simulation library (EasyDyn) is a C++ library, available freely and developed by the Theoretical Mechanics, Dynamics and Vibrations lab at the University of Mons [15]. The kinematic and the dynamic behavior of a mechanical system can be simulated based on configuration parameters and the expression of all forces applied on all bodies.

The library includes the following components:

- Vector algebra;
- Routines constructing the 3D models;
- Routines which solve second order differential equations;
- Numerical routines building the equations of motion.

Some detailed examples can be found in dedicated articles [14, 15].

2.2. CNC Feed Drive Model

The CNC model used in this work is based on the one proposed by Erkorkmaz (see Fig. 1) [8]. The current amplifier K_a transforms the control signal u to current i. The current is sent to the motor and is converted to motor torque T_m through the torque constant K_t. The motor torque T_m, from which the disturbance torque T_d is subtracted, gives the available torque on the motor shaft. The total inertia J reflected to the motor

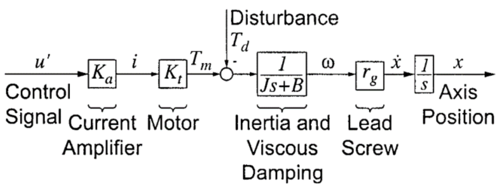

Fig. 1. Feed Drive Model [8]

shaft and the viscous damping B characterize the axis dynamic. The transmission ratio r_g multiplied by the rotation speed ω gives the linear speed of the table. The position x is then obtained by integrating the linear speed.

The Table 1 & 2 present, respectively, the constant parameters and the variable parameters of the model.

Table 1. Constant parameters of the feed drive model [6].

Parameter		Unit	X-axis	Y-axis
K_a	Current amplifier gain	[A/V]	6.4898	7.5768
K_t	Motor gain	[Nm/A]	0.4769	0.4769
J	Total reflected inertia	[kg.m²]	0.0077736	0.0098109
B	Viscous damping	[kg.m²/s]	0.019811	0.28438
r_g	Transmission gain	[mm/rad]	1.5915	1.5915

Table 2. Variable parameters of the feed drive model.

Parameter		Unit
u	Axis command	[V]
i	Motor current	[A]
T_m	Motor torque	[Nm]
T_d	Disturbance torque	[Nm]
ω	Motor shaft's rotation speed	[rad/s]
$\dot{x}$	Axis velocity	[mm/s]
x	Axis position	[mm]
s	Laplace multiplier	[1/s]

The constant parameter values in Table 1 come from the work of Yeung [6]. They correspond to a 3-axis milling machine (FADAL 2216). The axes are driven by DC motors. The cutting feed rate ranges from 0.25 mm/s to 10160 mm/s. The workspace dimensions are 559x406x508 mm (x-y-z).

2.3. Controller

The control structure used on the feed drive model is a PID controller which closes the position loop. Thus, the command of the system is no longer the parameter u, but the position x_r. A feedforward compensation is also applied to widen the servo tracking bandwidth (Fig. 2).

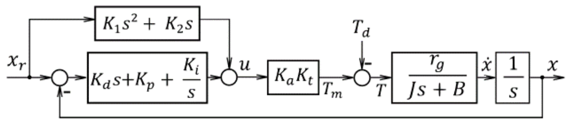

Fig. 2. Feed Drive with controller and feedforward compensation [16]

Parameters included in controller loops are presented in Table 3. They issue from an article which describes an identification technique for virtual CNC [16] and concern also the 3-axis milling machine (FADAL 2216).

The disturbance torque noted T_d combines the friction forces and cutting forces. A simple friction model, proposed by Erkorkmaz [16] is implemented in this framework. This model can easily be replaced by a more sophisticated one [17]. In such a case, the principal issue is to determine all parameters which constitute the model.

Table 3. Constant parameters of feed drive model [16].

Parameter		Unit	X-axis	Y-axis
K_d	Derivative gain	[V.s/mm]	0.3	0.278
K_p	Proportional gain	[V/mm]	500	462.539
K_i	Integral gain	[V/s.mm]	70	64.75
K_1	Feedforward on acceleration	[V.s²/mm]	0	0
K_2	Feedforward on speed	[V.s/mm]	-2.37E-6	5.55E-4

Concerning the cutting forces, they are estimated using a mechanistic model presented in section 3. Cutting forces are then included into the model as a disturbance torque acting on the motor axis.

3. Cutting forces simulation

Machining operations are complex to model due to the complex physical phenomena involved at the tool/chip interface (high strain, strain rates, temperatures …). At a macroscopic level, it is however possible to simplify the simulation by using analytical laws linking the cutting forces to macroscopic quantities such as depth of cut or undeformed chip thickness. A common approach used to model cutting forces in milling is to discretize the cutter along its axis in disc of elementary height d_a. On each disc, the cutting forces along a local frame oriented along cutting speed (index t), normal direction to the cutter (index r) and axial direction (index a) can be computed as

$$dF_i = K_{c,i} \, . \, h \, . \, d_a + K_{e,i} \, . \, dS \;(i = t, r, a)$$

where $K_{c,i}$ is specific pressure, h is the undeformed chip thickness, d_a is the height of the disc, $K_{e,i}$ is the coefficient of edge forces and dS the elementary length of the cutting edge. Engin and Altintas [18] made a complete description of the geometrical relation needed to project the local cutting forces in a global frame.

The computation of the undeformed chip thickness for complex trajectories can be achieved by the so-called 'eraser of matter' model [19]. This model is used in this paper to compute the cutting forces on a milling tool while machining the corner of a cavity.

4. Simulation results

The milling simulation of a 90° corner using a cylindrical endmill with four teeth is presented in this section. The situation is represented in Fig. 3. The raw material is Ti6Al4V and the machining parameters (listed in Table 4) are common values encountered on the literature for this material [20, 21]. Along the toolpath, the tool performs an entry into the material, passes through a corner and comes out of the material. The corner radius is equal to 20 mm for the smooth toolpath.

The aim of the simulation is to show the framework working all together (feed drive model + control loop + cutting forces) for a specific case with common values.

The toolpath is generated using the Velocity Profile Optimization (VPOp) software [2]. The kinematic characteristics of the modeled CNC are as follows:

- Maximum feed rate: 30 m/min on x-axis, 30 m/min on y-axis and 30 m/min on z-axis;
- Acceleration limits: 2.5 m/s² on x-axis, 3 m/s² on y-axis and 2.1 m/s² on z-axis;
- Jerk limits: 5 m/s³ on x-axis, 5 m/s³ on y-axis and 50 m/s³ on z-axis.

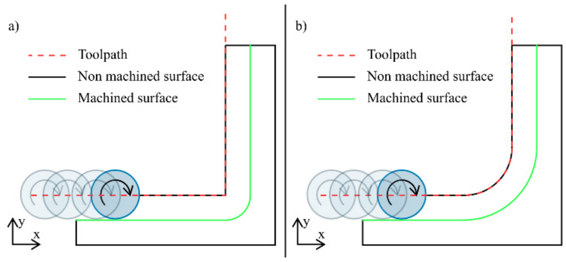

Fig. 3. Machining a 90° a) unsmooth corner b) smooth corner

Table 4. Machining parameters

Parameter		Unit	Value
D_c	Tool diameter	[mm]	10
a_e	Radial depth of cut	[mm]	5
Z	Number of teeth	[]	2
f_z	Feed per tooth	[mm/tooth]	0.2
a_p	Axial depth of cut	[mm]	3
f	Feed rate	[mm/min]	600
N	Rotation speed (clockwise)	[RPM]	1500
V_c	Cutting speed	[m/min]	47.12
Kct	Tangential specific pressure	[MPa]	550
Kcr	Radial specific pressure	[MPa]	200

The tangential feedrate, generated by considering the kinematic limits of the machine, is represented in Fig. 4.

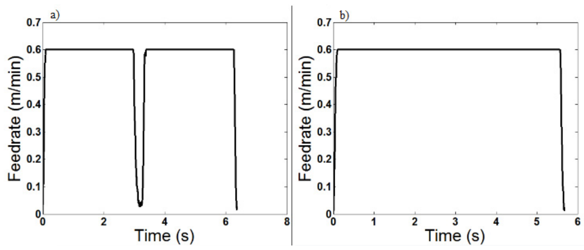

Fig. 4. Tangential feedrate for a) unsmooth corner b) smooth corner

In the Table 5, the length of the toolpaths, the theoretical times, the machining times and the difference between theoretical and machining times are listed. The theoretical time is obtained without considering the kinematic limits of the machine (admitting infinite accelerations). Thus the feedrate is considered as constant along the toolpath.

In the unsmooth toolpath (Fig. 4a), a sharp decrease of the feedrate is observed when approaching the corner, which explains that the difference between theoretical and machining time is higher in this case compared to the difference for the smooth toolpath. It highlights that angular toolpath sometimes produce by CAM software are not always ideal.

Table 5. Toolpaths characteristics

Toolpath	Length	Theoretical time	Machining time	Difference
Unsmooth	60.00 mm	6.000 s	6.366 s	6.10%
Smooth	55.71 mm	5.557 s	5.682 s	2.25%

For each simulation (unsmooth and smooth toolpath), the position, the velocity, the acceleration, the jerk and the difference between command and simulated response are presented. Only the results along the x-axis are presented since a similar trend can be observed for the y-axis.

4.1. Simulation without cutting forces acting on tool

In this section, a 90° corner trajectory without cutting forces is simulated. Results are presented in parallel for the unsmooth and the smooth trajectory.

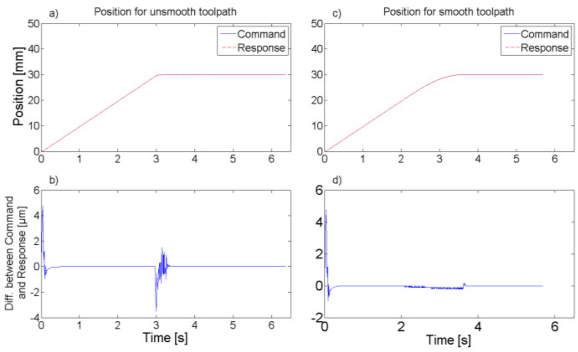

Fig. 5. Simulation without cutting forces: a) Commanded and simulated position for unsmooth toolpath; b) Difference between commanded and simulated position; c) Commanded and simulated position for smooth toolpath; d) Difference between commanded and simulated position

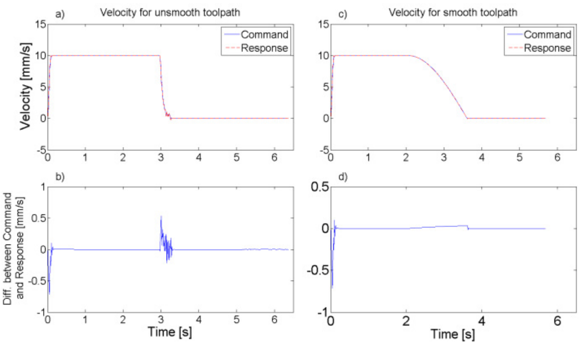

Fig. 6. Simulation without cutting forces: a) Commanded and simulated velocity for unsmooth toolpath; b) Difference between commanded and simulated velocity; c) Commanded and simulated velocity for smooth toolpath; d) Difference between commanded and simulated velocity

As presented in Fig. 5, the difference between set point and controlled position is relatively small. Similar results can be observed at the beginning of the trajectory (acceleration stage) for the unsmooth and the smooth trajectories. As seen in Fig. 5b, 5d, Fig. 6b, 6d, Fig. 7b, 7c and Fig. 8b, 8c, the errors found near the corner of the unsmooth trajectory are higher than those appearing in the smooth case.

A violation of feedrate is also noticed at the end of the acceleration stage, both for the smooth and the unsmooth trajectory. In Fig. 7, the acceleration command is violated but the response signal stays below the axis kinematic limit (acceleration limit on the x-axis is 2.5 m/s²). Concerning the jerk value (Fig. 8), a violation of the kinematic limit is noticed during the acceleration and deceleration stages, both for the smooth and unsmooth trajectory (jerk limit on x-axis is 5 m/s³).

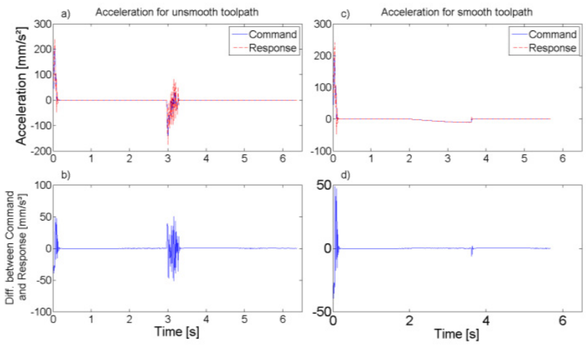

Fig. 7. Simulation without cutting forces: a) Commanded and simulated acceleration for unsmooth toolpath; b) Difference between commanded and simulated acceleration; c) Commanded and simulated acceleration for smooth toolpath; d) Difference between commanded and simulated acceleration

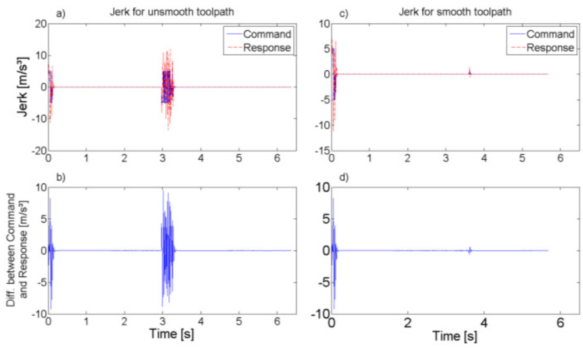

Fig. 8. Simulation without cutting forces: a) Commanded and simulated jerk for unsmooth toolpath; b) Difference between commanded and simulated jerk; c) Commanded and simulated jerk for smooth toolpath; d) Difference between commanded and simulated jerk

4.2. Simulation with cutting forces acting on tool

In this section, a 90° corner trajectory with cutting forces is simulated. Results are presented in parallel for the unsmooth and the smooth trajectory. As before, the difference between the position set point and the simulated motion is small (Fig. 9b and 9d). The observations concerning the velocity, the acceleration and the jerk are similar to the previous case. Moreover, the influence of cutting forces is clearly visible on the position, the velocity, the acceleration and the jerk graphics (Fig. 9b, 9d, Fig. 10b, 10d, Fig. 11b, 11d and Fig. 12b, 12d).

Both for the unsmooth and the smooth toolpath, the cutting forces values range between -340 N and 340 N, which are typical values for the milling process [9, 22, 23]. As seen in Fig. 13a, for the unsmooth trajectory, the cutting forces along the x-axis increases rapidly when the tool comes close the corner, followed by a sharp decrease due to the rapid slowdown of the tool. After that, the tool accelerates towards the y-axis and the change of direction is accomplished. For the smooth case, the change of direction is more continuous, as seen in Fig.

13b. In both cases, the trend of the force along x-axis before the corner is the same as the trend of the force along y-axis after the corner, and vice versa.

As represented in Fig. 3, the milling operation simulated in this work uses a climb milling strategy. The detailed profile of the cutting force presented in Fig. 14 corresponds the expected trend while using climb milling. Indeed, the forces along y-axis increase nearly instantaneously as the chip thickness is at its maximum rate when the tool enters in contact with the piece. Then, it decreases continuously as the direction of the tangential force changes during the rotation of the tool.

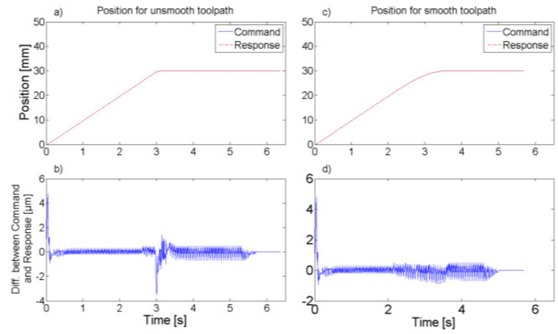

Fig. 9. Simulation considering cutting forces: a) Commanded and simulated position for unsmooth toolpath; b) Difference between commanded and simulated position; c) Commanded and simulated position for smooth toolpath; d) Difference between commanded and simulated position

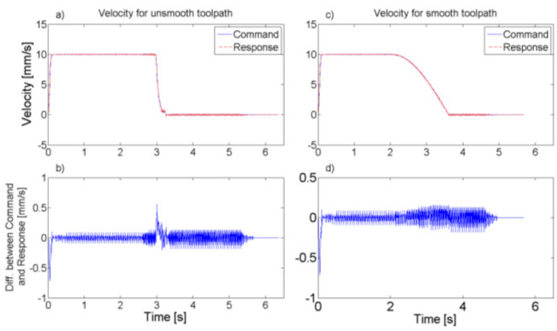

Fig. 10. Simulation considering cutting forces: a) Commanded and simulated velocity for unsmooth toolpath; b) Difference between commanded and simulated velocity; c) Commanded and simulated velocity for smooth toolpath; d) Difference between commanded and simulated velocity

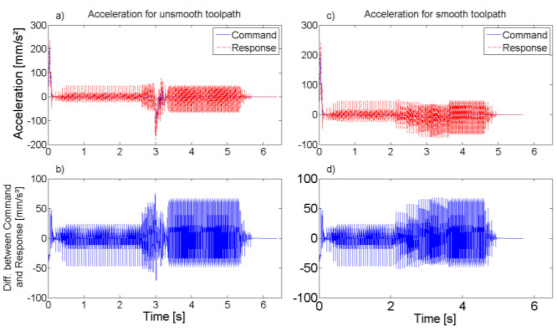

Fig. 11. Simulation considering cutting forces: a) Commanded and simulated acceleration for unsmooth toolpath; b) Difference between commanded and simulated acceleration; c) Commanded and simulated acceleration for smooth toolpath; d) Difference between commanded and simulated acceleration

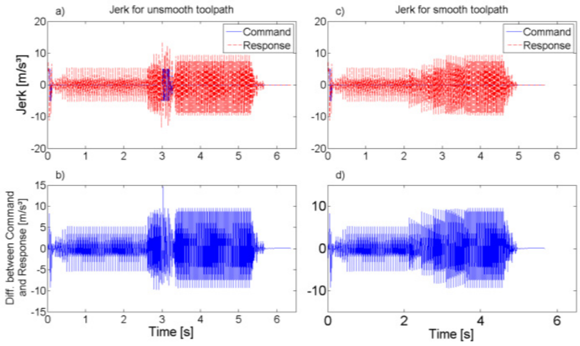

Fig. 12. Simulation considering cutting forces: a) Commanded and simulated jerk for unsmooth toolpath; b) Difference between commanded and simulated jerk; c) Commanded and simulated jerk for smooth toolpath; d) Difference between commanded and simulated jerk

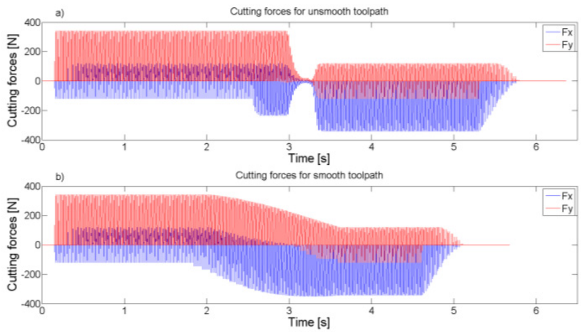

Fig. 13. Cutting forces for a) unsmooth trajectory; b) smooth trajectory

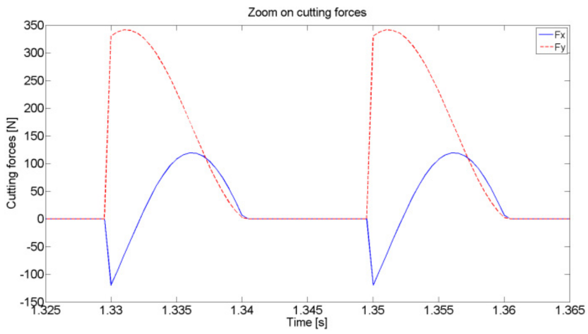

Fig. 14. Zoom on cutting forces

5. Conclusion

In this paper, a simulation framework combining the prediction of the cutting forces applied on a milling tool during a machining operation and the general behavior of a machine tool including its axis dynamics, its controller structure and its friction model has been presented. The cutting forces estimation is based on a method which discretizes the cutter along its axis in elementary discs. The general behavior of the machine tool and its control are simulated using a multibody simulation library.

To illustrate the simulation framework, a 90° corner trajectory has been simulated, using on the one hand an unsmooth toolpath and on the other hand a smooth toolpath. To highlight the impact of the cutting forces, a simulation without considering cutting forces has been compared to a simulation taking the cutting forces into account. For the case considering the cutting forces, we noticed an oscillation of position and velocity around controlled values instead of reaching exactly the commanded values as in the case where cutting forces had not been considered.

As a perspective for further works, different components forming the dynamic model (axis dynamic, controller, friction, …) could be replaced by more sophisticated models. Then, an important issue would be the model parameters identification.

Moreover, some experimental validations will be necessary to corroborate the simulation framework.

References

[1] Altintas Y, Brecher C, Weck M, Witt S. Virtual Machine Tool Keynote Paper of STC M. Annals of CIRP, 2005, 54/2, 651-674.

[2] Beudaert X. Open CNC : optimized interpolation for 5-axis high speed machining of complex surfaces. Mechanical engineering. Ecole normale supérieur de Cachan – ENS Cachan, 2013. French. <tel-00918816>

[3] Lavernhe S. Prise en compte des contraintes associées au couple MO-CN en génération de trajectoires 5 axes UGV. Engineering Sciences [physics]. Ecole normale supérieure de Cachan – ENS Cachan, 2006. French. <tel-00362983>

[4] Erkorkmaz K, Altintas Y. High speed CNC system design. Part I: Jerk limited trajectory generation and quintic spline interpolation. International Journal of Machine Tools and Manufacturing, 41(9) (2001) 1323-1345.

[5] Altintas Y. Manufacturing Automation: Metal Cutting Mechanics, Machine Tool Vibrations, and CNC Design. Cambridge University Press, Cambridge, 2000.

[6] Yeung C-H, Altintas Y, Erkorkmaz K. Virtual CNC system – Part I: System architecture. International Journal of Machine Tools and Manufacture, 46(10) (2006) 1107-1123.

[7] Altintas Y, Erkorkmaz K, Zhu W-H. Sliding mode controller design for high speed drives. Annals of CIRP 49(1) (2000) 256-270 .

[8] Erkorkmaz K. Optimal trajectory Generation and precision tracking control for multi-axis machines. Ph.D. Thesis. University of British Columbia, Department of Mechanical Engineering. BC, Canada..

[9] Rivière-Lorphèvre E, Filippi E, Dehombreux P. Chatter prediction using dynamic simulation. International Review of Mechanical Engineering (I.R.E.M.E.) (2007) 1(1)

[10] Pateloup V, Duc E, Ray P. Corner optimization for pocket machining. International Journal of Machine Tools and Manufacture 44(12–13) (2004), 1343–1353.

[11] Banerjee A, Feng H, Bordatchev E. Process planning for Floor machining of 2½D pockets based on a morphed spiral tool path pattern. Computers and Industrial Engineering archive, 63 (4) (2012), 971-979

[12] Bieterman M, Sandstrom D. A curvilinear tool-path method for pocket machining. Journal of Manufacturing Science and Engineering, Transactions of the ASME, 125(4) (2003), 709–715

[13] Hyunh H N, Rivière-Lorphèvre E, Verlinden O. Integration of machining simulation within multibody framework: application to milling. In Proceedings of the 4th Joint International Conference on Multibody System Dynamics, may – june 2016.

[14] Verlinden O, Kouroussis G, Conti C. EasyDyn: A framework based on free symbolic and numerical tools for teaching multibody systems. MULTIBODY DYNAMICS 2005 – ECCOMAS Thematic Conference (2005).

[15] Verlinden O, Ben Fékih L, Kouroussis G. Symbolic generation of the kinematics multibody systems in EasyDyn: From MuPAD to Xcas/Giac. Theoretical & applied mechanics letters 3, 013012 (2013).

[16] Erkorkmaz K, Wong W. Rapid identification technique for virtual CNC drives. International Journal of Machine Tools & Manufacture 47 (2007) 1381-1392.

[17] Prévot D. Modélisation avancée du couple Machine Outil/Commande Numérique dans un contexte UGV pour l'optimisation du calcul de trajectoires multi axes. Mechanical engineering. Ecole normale supérieure de Cachan – ENS Cachan, 2011. French. <tel-00764975>

[18] Engin S, Altintas Y. Mechanics and dynamics of general milling cutters. Part I: Helical ends mills. International Journal of Machine Tools and Manufacture, 41 (2001) 2195-2212.

[19] Peigne G et al. A model of milled surface generation for time domain simulation of high-speed cutting. Proc. Instn Mech. Engrs Part B : J. Engineering Manufacture, 217(7) (2003) 919-930

[20] Altintas Y, Lee P. A general mechanics and dynamics model for helical end mills. Annals of the CIRP 45(1) (1996) 59-64.

[21] Engin S, Altintas Y. Mechanics and dynamics of general milling cutters. Part I: helical end mills. International Journal of Machine Tools & Manufacture 41 (2001) 2195-2212.

[22] Rivière-Lorphèvre E, Barboza J, Filippi E, D'Alvise L. Cutting forces evaluation in milling using an analytical/finite element mixed approach. 11th CIRP Conference on Modeling of Machining Operations (2008).

[23] Engin S, Altintas Y. Mechanics and dynamics of general milling cutters. Part I: helical end mills. International Journal of Machine Tools & Manufacture 41 2195-2212 (2001).